Int. J. Solids Structures Vol. 26, No. 5/6, pp. 581–600, 1990
Printed in Great Britain.

0020–7683/90 $3.00 + .00

ANALYSIS OF INTERFACIAL THERMAL STRESSES AND ADHESIVE STRENGTH OF BI-ANNULAR CYLINDERS

E. Suhir and T. M. Sullivan
AT&T Bell Laboratories, Murray Hill, NJ 07974, U.S.A.

(*Received* 19 *April* 1989; *in revised form* 20 *July* 1989)

Abstract—An engineering theory for predicting interfacial stresses in finite bi-annular cylinders subjected to thermally induced or external loading is developed for the evaluation of epoxy molding compounds for plastic packaging of microelectronic devices. Bi-material co-axial cylindrical specimens are being used to characterize the adhesive strength of several molding compound candidates. With this theory, it is possible to calculate both shearing and normal (radial) stresses arising at the interface between an inner (adherend) and outer (adhesive) cylinder. Predictions for a pyrex(inner)-epoxy(outer) bi-annular cylinder agree well with the results from finite element analyses. It is concluded that bi-annular cylindrical specimens can be successfully applied to evaluate the adhesive strength of materials.

Although our theory has been developed for a specific materials science problem, it has a broad scope of applications. Examples include insulated tubes, electrical wires, coated optical fibers, high-pressure vessels, various shaft-hub joints, and even barrels of artillery guns.

INTRODUCTION

Bi-annular cylindrical structures are widespread in engineering. Examples are: insulated tubes and electrical wires, coated optical fibers, high-pressure vessels, barrels of artillery guns, and shaft-hub joints in gears, turbines and propellers. The problem of finding a complete solution for the three-dimensional elastic or thermoelastic equations of solid mechanics for such structures is one of extraordinary analytical difficulty (see, for instance, Filon (1902), Lurie (1955), Takeuti *et al.* (1983) and Hetnarski (1986)). Therefore, our analysis of bi-annular cylinders, when subjected to thermally induced and/or external shear loading, is based on more or less elementary methods of structural mechanics, rather than on rigorous approaches of mathematical physics.

In this study, emphasis is on the evaluation of interfacial stresses responsible for the adhesive strength of the cylinder. It is assumed that no special adhesive material is used, so that interfacial adhesive strength is due to the cylinder materials themselves. Obviously, this requires that at least one of these materials exhibits adhesive properties.

This analysis is performed in connection with an evaluation study of epoxy molding compounds for microelectronics packaging. In this study co-axial cylindrical specimens are being used to characterize the adhesive strength of the candidate materials. The inner cylinders in these specimens are made of nickel, copper or gold-plated nickel, while the outer cylinders are composed of the epoxy materials under evaluation. All of the epoxies are expected to have good adhesive properties. In order to perform experimental photoelastic stress analysis (ASTM F-100), we also include specimens whose inner cylinders are made of pyrex.

Typical bi-material co-axial specimens are shown in Fig. 1 as they appear prior to testing (pyrex inserts are shown in this picture). The shearing force necessary to overcome adhesion and friction between the two materials is applied using an Instron machine with specially designed fixtures. During testing, these fixtures and a test specimen are arranged as shown by the schematic cross-section in Fig. 2. Figure 3 is a photograph of the fixtures and also shows three specimens after having been tested. Compressive loading during testing is applied at a constant strain rate until the adhesion between the two materials breaks down. Figure 4 illustrates the important features of a typical force vs. time printout obtained from each test. Total shear-off force can be described as the sum of the interfacial adhesive strength and a frictional force, which is due to the thermally induced lateral interfacial pressure.

The main purpose of the analysis below is to determine the shearing and the normal (radial) interfacial stresses due to the thermal contraction mismatch of the materials, as well as the interfacial shearing stresses caused by external shear loading. The analytical model which is developed enables one to evaluate the mechanical performance of adhesively bonded bi-annular cylindrical structures and test specimens under the combined action of thermal and external loading.

THEORY

1. *Basic equations*

Let a bi-annular circular cylinder of finite length be fabricated at an elevated temperature and subsequently cooled down by the temperature Δt. This generates distributed shearing $\tau(z)$ and radial $p(z)$ stresses acting at the interface of the inner and the outer cylinders and caused by the thermal contraction mismatch of the cylinder materials.

If the stresses $\tau(z)$ and $p(\tau)$ were known, then the axial $w(z)$ and the radial $u(z)$ interfacial displacements of the component cylinders could be evaluated by the following approximate formulas:

$$\left.\begin{aligned} w_0(z) &= -\alpha_0 \Delta t z + \lambda_0 \int_0^z T(\zeta)\,\mathrm{d}\zeta - \kappa_0 \tau(z) - \mu_0 \int_0^z p(\zeta)\,\mathrm{d}\zeta \\ w_1(z) &= -\alpha_1 \Delta t z - \lambda_1 \int_0^z T(\zeta)\,\mathrm{d}\zeta + \kappa_1 \tau(z) + \mu_1 \int_0^z p(\zeta)\,\mathrm{d}\zeta \end{aligned}\right\} \tag{1}$$

$$\left.\begin{aligned} u_0(z) &= -\alpha_0 \Delta t r_1 - \delta_0 r_1 p(z) - \gamma_0 r_1 T(z) \\ u_1(z) &= -\alpha_1 \Delta t r_1 + \delta_1 r_1 p(z) - \gamma_1 r_1 T(z) \end{aligned}\right\}. \tag{2}$$

Here $w_0(z)$ and $w_1(z)$ are the axial interfacial displacements of the inner and the outer cylinders, respectively, $u_0(z)$ and $u_1(z)$ are the radial interfacial displacements.

$$T(z) = \int_{-l}^{z} \tau(\zeta)\,\mathrm{d}\zeta \tag{3}$$

is the axial force at the given cross-section z, l is half the cylinder's length, α_0 and α_1 are coefficients of thermal expansion of the cylinder materials ($\alpha_1 > \alpha_0$),

$$\lambda_0 = \frac{1}{\pi E_0 (r_1^2 - r_0^2)}, \quad \lambda_1 = \frac{1}{\pi E_1 (r_2^2 - r_1^2)} \tag{4}$$

are the axial compliances of the cylinders, r_0 is the inner radius of the inner cylinder, r_1 is the interfacial radius, r_2 is the outer radius of the bi-annular (outer) cylinder, E_0 and E_1 are Young's moduli of the materials,

$$\left.\begin{aligned} \kappa_0 &= \frac{r_1}{E_0} \frac{r_1^2 - \bar{r}_0^2 + 2(1+\nu_0) r_0^2 \ln \dfrac{r_1}{\bar{r}_0}}{r_1^2 - r_0^2}, \quad \bar{r}_0 = \frac{r_0 + r_1}{2} \\ \kappa_1 &= \frac{r_1}{E_1} \frac{\bar{r}_2^2 - r_1^2 + 2(1+\nu_1) r_2^2 \ln \dfrac{\bar{r}_2}{r_1}}{r_2^2 - r_1^2}, \quad \bar{r}_2 = \frac{r_1 + r_2}{2} \end{aligned}\right\} \tag{5}$$

are the interfacial axial compliances of the cylinders (Appendix A), ν_0 and ν_1 are Poisson's ratios of the materials,

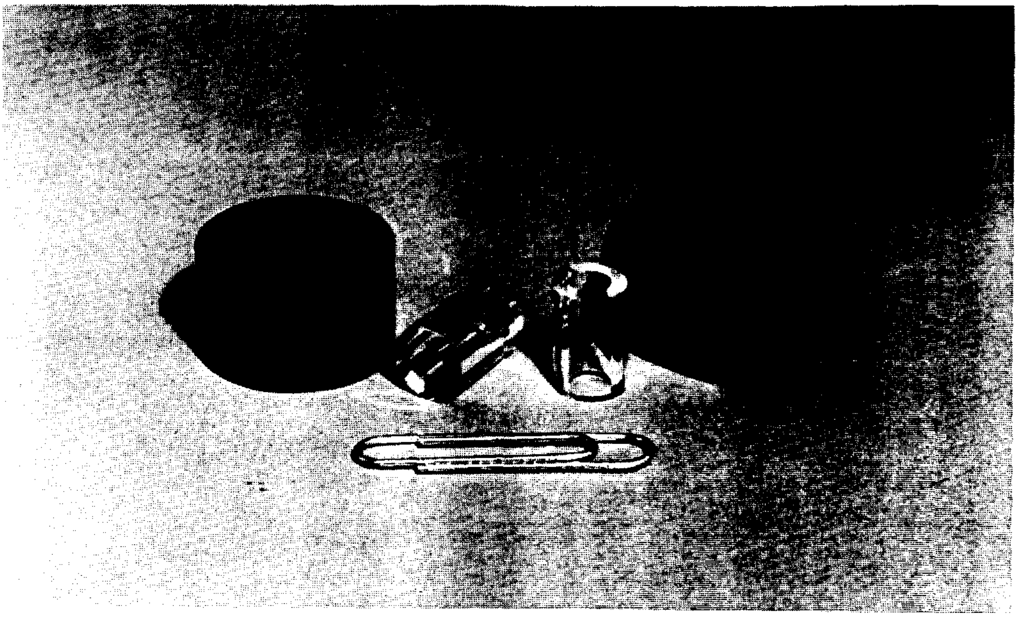

Fig. 1.

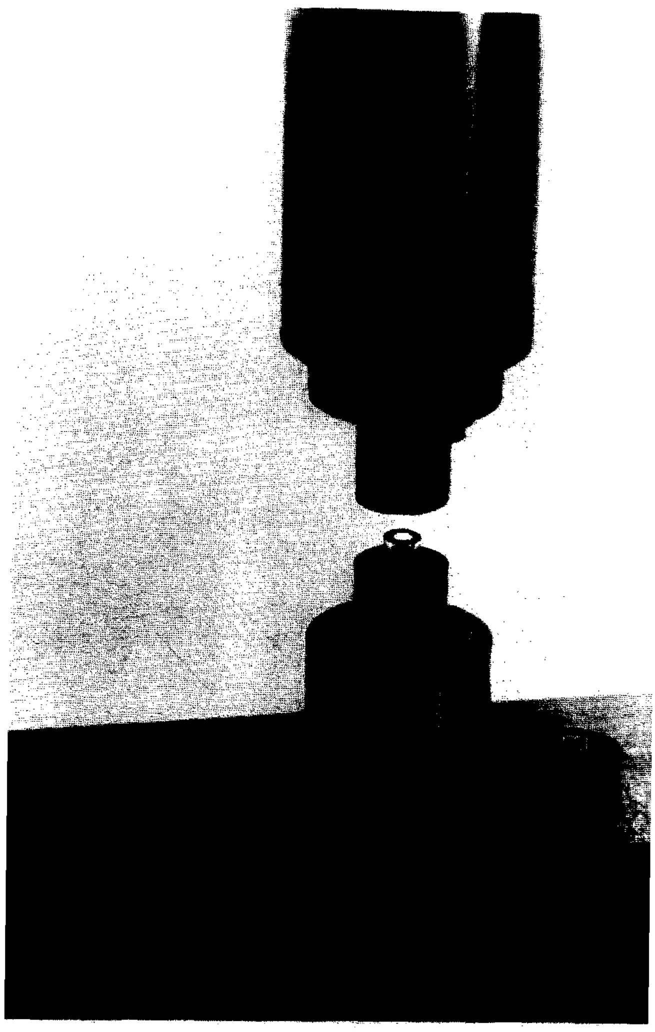

Fig. 3.

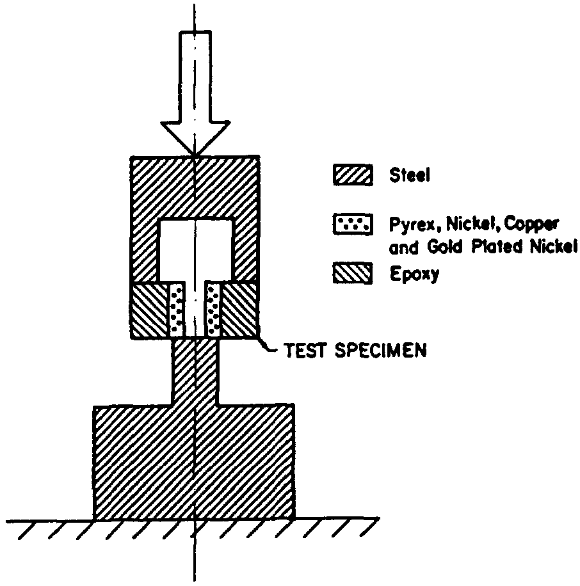

Fig. 2.

$$\mu_0 = \frac{2\nu_0}{E_0}\frac{r_1^2}{r_1^2-r_0^2}, \quad \mu_1 = \frac{2\nu_1}{E_1}\frac{r_1^2}{r_2^2-r_1^2} \tag{6}$$

are the compliance factors for the axial displacements with respect to the lateral pressure (Appendix B),

$$\gamma_0 = \nu_0\lambda_0 = \frac{\nu_0}{\pi E_0(r_1^2-r_0^2)}, \quad \gamma_1 = \nu_1\lambda_1 = \frac{\nu_1}{\pi E_1(r_2^2-r_1^2)} \tag{7}$$

are the compliance factors for the radial displacements with respect to the axial force $T(z)$ (Appendix C), and δ_0 and δ_1 are the compliance factors for the radial displacements with respect to the lateral pressure. The latter factors should be calculated by the formulas (Appendix C)

$$\delta_0 = \frac{(1-\nu_0)r_1^2+(1+\nu_0)r_0^2}{E_0(r_1^2-r_0^2)}, \quad \delta_1 = \frac{(1-\nu_1)r_1^2+(1+\nu_1)r_2^2}{E_1(r_2^2-r_1^2)} \tag{8}$$

for relatively short ("disc-like") cylinders, when a plane stress approximation is applicable, or by the formulas

$$\delta_0 = \frac{1+\nu_0}{E_0}\frac{(1-2\nu_0)r_1^2+r_0^2}{r_1^2-r_0^2}, \quad \delta_1 = \frac{1+\nu_1}{E_1}\frac{(1-2\nu_1)r_1^2+r_2^2}{r_2^2-r_2^2} \tag{9}$$

in the case of sufficiently long ("tube-like") cylinders, when a plane strain approximation should be used. For some geometries, the aspect ratios of the inner and outer cylinders may be such that the factor δ_0 should be evaluated by the plane strain formula, while the factor δ_1 should be determined on the basis of the plane stress formula. The difference in the numerical results is small, however, in any event. The origin of the coordinates r, z is located at the middle of the cylinder axis.

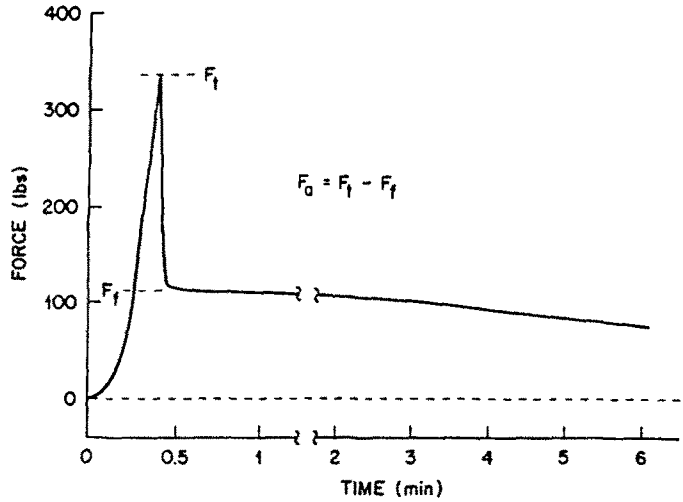

Fig. 4.

The first terms in (1) and (2) are unrestricted thermal contractions. The second terms in (1) are axial interfacial displacements caused by the forces $T(z)$ and evaluated under an assumption that these forces are uniformly distributed over the cylinder cross-sections. The third terms in (1) account for the non-uniform distribution of the forces $T(z)$ and reflect an assumption that the corresponding corrections depend only on the shearing force in the given cross-section and are not affected by forces acting in other cross-sections. The last terms in (1) are due to the lateral pressure $p(z)$. The second terms in the formulas (2) are radial interfacial displacements due to the lateral pressure $p(z)$, and the third terms account for the additional radial displacements caused by the axial forces $T(z)$. The derivations of the formulas for the above components of the axial and radial interfacial displacements are given in Appendices B and C. Note that a similar approach was taken in an approximate stress analysis of bi-metal thermostats (Suhir, 1986).

Conditions for the compatibility of displacements require that the axial interfacial displacements of the inner cylinder be equal to the axial displacements of the outer cylinder, and that the radial interfacial displacements of the inner cylinder be equal to the radial displacements of the outer cylinder:

$$w_0(z) = w_1(z); \quad u_0(z) = u_1(z). \tag{10}$$

Substituting (1) and (2) into (10) we obtain the following basic equations for the unknown stress functions $\tau(z)$ and $p(z)$:

$$\kappa\tau(z) - \lambda \int_0^z T(\zeta)\,\mathrm{d}\zeta - \mu \int_0^z p(\zeta)\,\mathrm{d}\zeta = \Delta\alpha\Delta tz \tag{11}$$

$$\delta p(z) + \gamma T(z) = \Delta\alpha\Delta t \tag{12}$$

where the following notation is used:

$$\lambda = \lambda_0 + \lambda_1, \quad \kappa = \kappa_0 + \kappa_1, \quad \mu = \mu_0 + \mu_1, \quad \delta = \delta_0 + \delta_1, \quad \gamma = \gamma_0 + \gamma_1, \quad \Delta\alpha = \alpha_1 - \alpha_0. \tag{13}$$

2. *Solutions to the basic equations*

Solving (12) for the function $p(z)$ and substituting the obtained expression into (11) we have:

$$\tau(z)-k^2\int_0^z T(\zeta)\,d\zeta = C_0\Delta\alpha\Delta tz \tag{14}$$

where the eigenvalue k and the constant C_0 are expressed by the formulas:

$$k=\sqrt{\frac{\lambda\delta-\mu\gamma}{\delta\kappa}},\quad C_0=\frac{\delta+\mu}{\delta\kappa}. \tag{15}$$

The integral equation (14) contains just one unknown function—the interfacial shearing stress $\tau(z)$.

Differentiating (14) by z, we obtain:

$$\tau'(z)-k^2T(z) = C_0\Delta\alpha\Delta t. \tag{16}$$

Obviously, when the cylinder is subjected to thermal loading only, no axial forces act at its end cross-sections $z = l$ and therefore the force $T(z)$ must be zero at the ends: $T(l) = 0$. This leads to the following boundary condition for the function $\tau(z)$:

$$\tau'(l) = C_0\Delta\alpha\Delta t. \tag{17}$$

The differentiation of the eqn (16) yields:

$$\tau''(z)-k^2\tau(z) = 0. \tag{18}$$

This simple homogeneous equation has the following solution:

$$\tau(z) = C\sinh kz+D\cosh kz \tag{19}$$

where C and D are constants of integration. The function $\tau(z)$ must be anti-symmetric with respect to the origin $z = 0$. Since, however, cosh kz is a symmetric function, we put the constant D equal to zero. Then we have:

$$\tau(z) = C\sinh kz. \tag{20}$$

Introducing (20) into (17) we obtain the following formula for the constant C:

$$C = C_0\frac{\Delta\alpha\Delta t}{k\cosh kl}. \tag{21}$$

Thus, the interfacial shearing stress is expressed as

$$\tau(z) = \tau_{max}\chi_\tau(z), \tag{22}$$

where

$$\tau_{max} = \tau(l) = C_0 \frac{\Delta\alpha\Delta t}{k} \tanh kl \tag{23}$$

is the maximum shearing stress at the end cross sections $z = \pm l$, and the function

$$\chi_\tau(z) = \frac{\sinh kz}{\sinh kl}, \quad 0 < \chi_\tau < 1, \tag{24}$$

characterizes the distribution of the interfacial shearing stress along the cylinder.

When the kl value is large enough (say, greater than 3.5), the eqns (22) and (23) can be simplified:

$$\tau(z) = \tau_{max}\, e^{-k(l-z)}, \quad \tau_{max} = C_0 \frac{\Delta\alpha\Delta t}{k}. \tag{25}$$

These formulas indicate that the maximum shearing stresses for sufficiently long (large l values) cylinders with stiff interfaces (large k values) are independent of the cylinder length and drop exponentially with decreasing z, i.e., they concentrate near the ends of the cylinder.

In another extreme case, when the kl value is small (say, smaller than 0.1), i.e. in the case of a "disc-like" cylinder, the formulas (22) and (23) yield:

$$\tau = C_0 \Delta\alpha\Delta t z. \tag{26}$$

Hence, for short cylinders with sufficiently compliant interfaces the shearing stress is linearly distributed along the cylinder.

Note, that if the effect of lateral pressure on the shearing stress were not considered ($\mu = 0$), then the formulas (15) would result in the following equations for the eigenvalue k and the shearing stress factor C_0:

$$k = \sqrt{\frac{\lambda}{\kappa}}, \quad C_0 = \frac{1}{\kappa}. \tag{27}$$

This k value is greater and the C_0 value is smaller than the corresponding values determined by (15). Hence, as evident from (25), not taking into account the effect of the lateral pressure results in smaller shearing stresses, which, in addition, are distributed over a smaller region than the stresses determined on the basis of the more general formulas (15).

After substituting (20) into (3) we find, that the axial shearing force is expressed as:

$$T(z) = -T_0 \chi_T(z) \Delta\alpha\Delta t \tag{28}$$

where

$$T_0 = \frac{C_0}{k^2} = \frac{\delta+\mu}{k^2\delta\kappa} = \frac{\delta+\mu}{\lambda\delta-\mu\gamma} \tag{29}$$

and the function

$$\chi_T(z) = 1 - \frac{\cosh kz}{\cosh kl} \tag{30}$$

characterizes the distribution of the force $T(z)$ along the cylinder.

When the kl value is large ("tube-like" cylinders), the factor $\chi_T(z)$ can be expressed by a simplified formula:

$$\chi_T(z) = 1 - e^{-k(l-z)}. \tag{31}$$

As evident from this formula, for small z values, i.e. for the cross-sections remote from the cylinder ends, the function $\chi_T(z)$ is close to unity, and the force $T(z)$ is independent of the location of the given cross-section z along the cylinder. Near the ends, where the z coordinate is on the same order as l, this force rapidly drops and turns to zero at the edges. In the case of a very short ("disc-like") cylinder, the function $\chi_T(z)$ can be presented as

$$\chi_T(z) = \frac{k^2}{2}(l^2 - z^2). \tag{32}$$

Hence, the force $T(z)$ changes in this case in accordance with a parabolic law.

The maximum shearing force occurs at the mid-cross-section and is

$$T(0) = T_{\max} = -T_0 \chi_T(0) \Delta\alpha \Delta t \tag{33}$$

where

$$\chi_T(0) = \chi_{\max} = 1 - \frac{1}{\cosh kl}. \tag{34}$$

For sufficiently long cylinders $(l \to \infty)$ $\chi_T(0) \cong 1$. For short cylinders when $\cosh kl \cong 1 + \frac{1}{2}(kl)^2$, the factor $\chi_T(0)$ is $\chi_T(0) \cong \frac{1}{2}(kl)^2$.

The radial pressure can be determined by introducing (28) into (12). This leads to an equation:

$$p(z) = p(l)\chi_p(z) \tag{35}$$

where

$$p(l) = \frac{\Delta\alpha \Delta t}{\delta} \tag{36}$$

is the radial pressure at the end cross-sections, and the function

$$\chi_p(z) = 1 + c\chi_T(z), \quad c = \frac{\gamma}{k^2} C_0 = \gamma \frac{\delta + \mu}{\lambda\delta - \mu\gamma} \tag{37}$$

characterizes the longitudinal distribution of the radial pressure.

For long enough cylinders, when the χ_T value is close to unity, the function $\chi_p(z)$ takes the greatest value, which is $\chi_p = 1 + c$, and the radial pressure is equal to

$$p_0 = (1+c)p(l) \tag{38}$$

for almost the entire cylinder. Only at the very ends this pressure decreases to the $p(l)$ value. For very short cylinders the factor χ_{max} is small and the factor χ_p is close to unity, so that the interfacial pressure is equal to $p(l)$ throughout the cylinder.

Note, that if the effect of the shearing stress on the radial pressure were not taken into account ($\gamma = 0$), then, as evident from (37), the factor χ_p would be close to unity and the interfacial pressure would become uniform and equal to $p(l)$ throughout the cylinder, as in the case of a small-length cylinder.

The total lateral force due to the normal pressure $p(z)$ is

$$P_n = 4\pi r_1 \int_0^l p(z)\,\mathrm{d}z = \frac{4\pi r_1}{k} p(l)[(1+c)kl - c\tanh kl]. \tag{39}$$

For long cylinders this formula can be simplified to:

$$P_n \cong 4\pi(1+c)p(l)r_1 l. \tag{40}$$

For short cylinders the formula (39) yields:

$$P_n = 4\pi p(l)r_1 l. \tag{41}$$

Thus, the total lateral force increases with an increase in the cylinder length. In the case of a very long cylinder this force is greater than in the case of a short cylinder by the factor of $1+c$.

3. *External shear loading*

Unlike thermally induced shearing stress, the shearing stress due to the external shear loading is symmetric with respect to the origin (Fig. 6a and b). In this case it is the constant C in the solution (19) which should be put equal to zero, so that this solution can be sought in the form:

$$\tau(z) = D\cosh kz. \tag{42}$$

Then the axial force at cross-section z is

$$T(z) = \int_{-l}^{z} \tau(z)\,\mathrm{d}z = \frac{D}{k}(\sinh kl + \sinh kz). \tag{43}$$

Introducing this equation into the boundary condition

$$T(l) = \frac{F_a}{2\pi r_1} \tag{44}$$

where F_a is the external shear force at the end plane of the cylinder, we have:

$$D = \frac{kF_a}{4\pi r_1 \sinh kl}. \tag{45}$$

Then eqn (43) yields:

$$T(z) = \frac{F_a}{4\pi r_1}\chi_T^e(z). \tag{46}$$

Here the function

$$\chi_T^e(z) = 1 + \frac{\sinh kz}{\sinh kl} \tag{47}$$

reflects the distribution of the force $T(z)$ along the cylinder.

Obviously, for each of the component cylinders, the axial force is zero at one end, is expressed by the formula (44) at the other end, and, based on symmetry considerations, must be twice as small as the $T(l)$ value in the middle of the cylinder:

$$T(-l) = 0, \quad T(0) = \frac{F_a}{4\pi r_1}, \quad T(l) = \frac{F_a}{2\pi r_1}. \tag{48}$$

Introducing (45) into (42) we obtain the following formula for the shearing stress:

$$\tau(z) = \tau_{\max}\chi_\tau^e(z) \tag{49}$$

where

$$\tau_{\max} = \tau(l) = \frac{kF_a}{4\pi r_1}\text{cotanh } kl \tag{50}$$

is the maximum stress (at the end cross-sections), and the function

$$\chi_\tau^e(z) = \frac{\cosh kz}{\cosh kl} \tag{51}$$

characterizes the longitudinal distribution of the shearing stress. Note, that unlike thermally induced shearing stress, the stress caused by the external shear loading is not zero at the mid-cross-section $z = 0$:

$$\tau(0) = \frac{kF_a}{4\pi r_1 \sinh kl} = \frac{\tau_{\max}}{\cosh kl}. \tag{52}$$

However, for long enough cylinders with stiff interfaces (large kl values) this stress in the mid-cross-section is very small. The maximum shearing stress in such cylinders is independent of the cylinder length and, as follows from (50), is expressed by the formula:

$$\tau_{\max} = \frac{kF_a}{4\pi r_1}. \tag{53}$$

The function $\chi_\tau^e(z)$ for long-and-stiff cylinders can be presented as

$$\chi_\tau^e(z) \cong e^{-k(l-z)}. \tag{54}$$

This formula indicates that the shearing stress concentrates near the cylinder ends and drops exponentially with the decrease in the coordinate z. Thus, for sufficiently long cylinders the distribution of the shearing stress due to an external shearing force is similar to the distribution of the thermally induced shearing stress.

For short cylinders the function χ_T^e which characterizes the longitudinal distribution of the axial force is close to 2, and the formula (46) yields:

$$T(z) \cong \frac{F_a}{2\pi r_1}. \tag{55}$$

Hence, the shearing stress in short cylinders is uniformly distributed over their lengths and can be evaluated by the formula

$$\tau \cong \frac{T}{2}l = \frac{F_a}{4\pi r_1 l}. \tag{56}$$

If a bi-annular cylinder experiences both thermally induced and external loading, then the total shearing stress can be evaluated as superposition of the solutions (22) and (49):

$$\tau(z) = \tau^T_{\max}\frac{\sinh kz}{\sinh kl} + \tau^e_{\max}\frac{\cosh kz}{\cosh kl}. \tag{57}$$

Here $\tau^T_{\max}$ is the maximum thermal shearing stress expressed by (23), and $\tau^e_{\max}$ is the maximum shearing stress due to the external loading and expressed by (50). As evident from (57), the maximum total shearing stress is

$$\tau(l) = \tau^T_{\max} + \tau^e_{\max} \tag{58}$$

at one end of the cylinder, and is

$$\tau(-l) = -\tau^T_{\max} + \tau^e_{\max} \tag{59}$$

at the other end (Fig. 6a and b).

If destructive shear-off tests are performed and the measured total and frictional forces are F_t and F_f, respectively (Fig. 4), then the adhesive force F_a can be obtained as $F_a = F_t - F_f$. The ultimate maximum shearing stress that the interface is able to withstand can be calculated by the formula (58). As a by-product, the coefficient of friction between the cylinder materials can be determined:

$$f = \frac{F_f}{P_n}. \tag{60}$$

Here P_n is the total force due to the normal thermally induced pressure. This force can be calculated by (39).

NUMERICAL EXAMPLE

We carry out a numerical example for a bi-annular cylinder, where the inner cylinder is made of pyrex ($E_0 = 9.1 \times 10^6$ psi $= 6.278 \times 10^{10}$ Pa, $\nu_0 = 0.2$, $\alpha_0 = 2.8 \times 10^{-6}$ 1/°C) and the outer cylinder is fabricated of epoxy ($E_1 = 2.1 \times 10^{-6}$ psi $= 1.449 \times 10^{10}$ Pa, $\nu_1 = 0.35$, $\alpha_1 = 22.0 \times 10^{-6}$ 1/°C). The inner, interfacial and outer radii of the cylinder are $r_0 = 0.094$ in $= 2.39$ mm, $r_1 = 0.175$ in $= 4.44$ mm and $r_2 = 0.4375$ in $= 11.112$ mm, respectively. The half length of the cylinder is $l = 0.250$ in $= 6.35$ mm, and the change in temperature is $\Delta t = 150$°C.

Table 1

1/lb	$\lambda_0 = 1.6054 \times 10^{-6}$	$\lambda_1 = 0.9428 \times 10^{-6}$	$\lambda = 2.5482 \times 10^{-6}$
(1/N)	(3.6115×10^{-7})	(2.1208×10^{-7})	(5.7323×10^{-7})
in^3/lb	$\kappa_0 = 1.5989 \times 10^{-8}$	$\kappa_1 = 18.2679 \times 10^{-8}$	$\kappa = 19.8669 \times 10^{-8}$
(m^3/N)	(5.8882×10^{-14})	$(67.2502 \times 12^{-14})$	$(73.1384 \times 10^{-14})$
in^2/lb	$\mu_0 = 6.1781 \times 10^{-8}$	$\mu_1 = 6.3493 \times 10^{-8}$	$\mu = 12.5274 \times 10^{-8}$
(m^2/N)	(8.9574×10^{-12})	(9.2057×10^{-12})	$(18.1631 \times 10^{-14})$
in^2/lb	$\delta_0 = 1.6468 \times 10^{-7}$	$\delta_1 = 8.0204 \times 10^{-7}$	$\delta = 9.6672 \times 10^{-7}$
(m^2/N)	(2.3877×10^{-12})	$(11.6286 \times 10^{-12})$	$(14.0163 \times 10^{-12})$
1/lb	$\gamma_0 = 3.2108 \times 10^{-7}$	$\gamma_1 = 3.2998 \times 10^{-7}$	$\gamma = 6.5106 \times 10^{-7}$
(1/m)	(7.2154×10^{-8})	(7.4149×10^{-8})	(14.6303×10^{-8})

$\Delta\alpha\Delta t = 0.00288$, $k = 3.5216$ 1/in $= 138.72$ 1/m.
$C_0 = 5685767$ lb/in^3 $= 1.55438 \times 10^{12}$ N/m^3, $C = 3290$ psi $= 22.697 \times 10^6$ Pa.
$\tau_{max} = 3286$ psi $= 22.669 \times 10^6$ Pa, $p(l) = 2979$ psi $= 20.551 \times 10^6$ Pa, $c = 0.2985$.
$\chi_{max} = 0.2927$, $p(0) = p_{max} = 3239$ psi $= 22.345 \times 10^6$ Pa.

Calculated values for the major parameters affecting the magnitude and the distribution of the interfacial stresses $\tau(z)$ and $p(z)$ are shown in Table 1. The factors δ_0 and δ_1 for the interfacial compliance of the cylinders in the radial direction are calculated by the plane strain formulas.

The calculated stresses $\tau(z)$ and $p(z)$ are plotted in Fig. 5a, where the results of the finite-element analysis are also indicated. The analytical and numerical data are in fairly good agreement, especially for the shearing stress.

If the influence of the lateral pressure on the shearing stress were not considered ($\mu = 0$), then the maximum shearing stress would be $\tau_{max} = 2939$ psi (20.275×10^6 Pa), which is about 10% smaller than the value obtained by taking this influence into account. If the effect of the shearing stress on the lateral pressure were not considered ($\gamma = 0$), then this pressure would be constant along the interface and equal to $p(l) = 2979$ psi (20.551×10^6 Pa). The calculated pressure in the middle of the cylinder, when this effect was taken into account, is about 8% greater.

If the value of kl becomes greater than, say, 3.5, then the tanh kl and χ_{max} values are very close to unity, and the interfacial stresses cease to increase with a further increase in the length of the cylinder. In the above example this takes place when the half length of the cylinder is about 1 in (25.4 mm). The calculated maximum values of the shearing and the normal radial stresses for $l = 1$ in are $\tau_{max} = 4650$ psi (32.079×10^6 Pa) and $p_{max} = 3740$ psi (25.801×10^6 Pa). The distribution of the calculated interfacial stresses for a 2 in long cylinder is shown in Fig. 5b. The agreement between the analytical and FEM results is quite good, especially for shearing stresses.

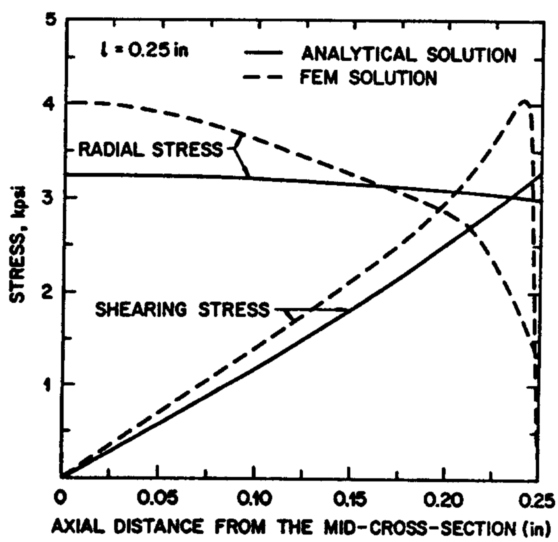

Fig. 5a.

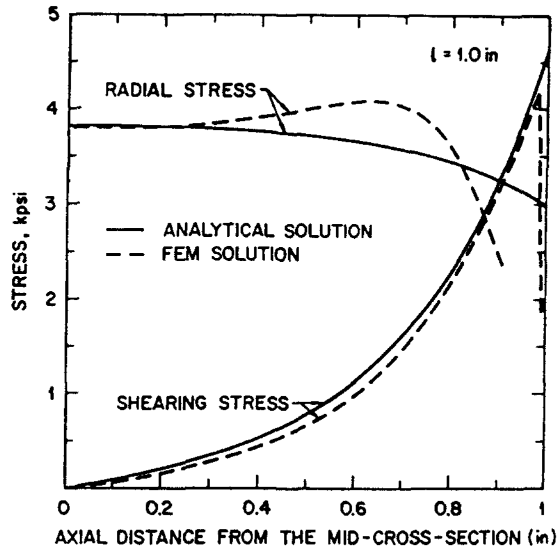

Fig. 5b.

The measured total and frictional forces during shear-off Instron tests (Fig. 4) are $F_t = 345$ lb (1535 N) and $F_f = 122$ lb (543 N). Thus, the ultimate adhesive force calculated as a difference $F_a = F_t - F_f$ is $F_a = 223$ lb (992 N). The calculated maximum shearing stresses at the end cross-sections due to the force F_a is $\tau_{\max} = 505$ psi (3.484×10^6 Pa). The total maximum shearing stress due to the combined thermal and external loading is therefore 3791 psi (26.153×10^6 Pa). The evaluated maximum thermally induced stress in this example is about 6.5 times greater than the maximum stress caused by external loading.

The calculated total lateral force due to the normal thermally induced pressure is $P_n = 1341$ lb (5967 N), and the calculated coefficient of friction between pyrex and epoxy is $f = 0.091$.

The distributions of the shearing stresses due to the external and thermally induced loading, as well as the total stresses, are shown in Fig. 6a and Fig. 6b for cylinders, whose lengths are 0.5 in (12.7 mm) and 2.0 in (50.8 mm), respectively. These figures indicate that in short cylinders the shearing stress due to external loading is rather uniformly distributed along the cylinder, while the thermal shearing stress varies linearly. When the

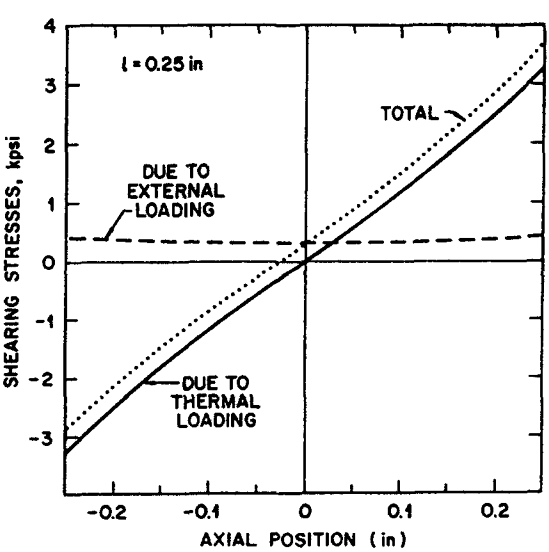

Fig. 6a.

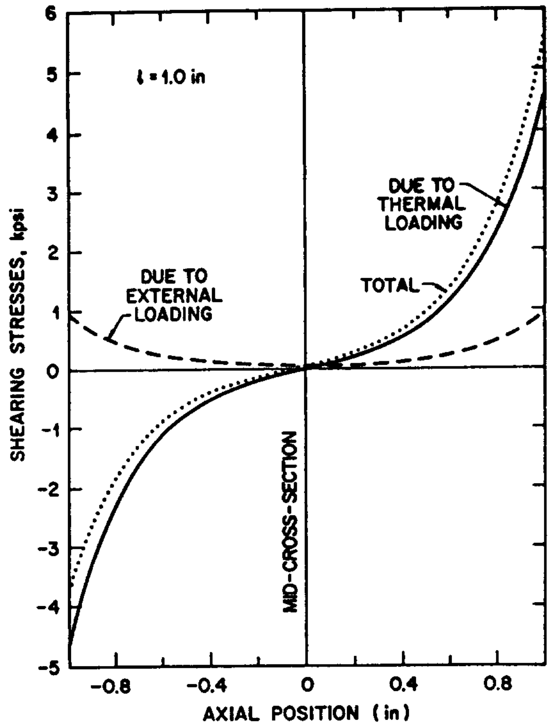

Fig. 6b.

cylinder length is increased, both stress categories decrease in the mid-portion of the cylinder and increase towards the ends. In sufficiently long cylinders the stresses concentrate at the cylinder ends.

CONCLUSIONS

The following major conclusions can be drawn from the executed analysis.

An engineering theory for predicting interfacial stresses in finite bi-annular cylinders subjected to thermally induced and/or external shear loading is developed. It is aimed primarily at the evaluation of the mechanical behavior of bi-material co-axial cylindrical specimens, used to characterize the adhesive strength of polymeric materials. No special adhesive is employed, so that the interfacial adhesive strength is due to the polymeric material itself. However, this theory can be easily modified if such a "special adhesive" is applied.

The *thermally induced shearing stresses* at the interface are anti-symmetric with respect to the mid-cross-section of the cylinder. They are zero in this cross-section and increase in magnitude when approaching the cylinder ends. For relatively short ("disc-like") cylinders with sufficiently compliant interfaces, the shearing stresses are distributed linearly along the cylinder, and the maximum values of these stresses are proportional to the length of the cylinder. In another extreme case, for long enough ("tube-like") cylinders with relatively stiff interfaces, the shearing stresses concentrate near the cylinder ends, and their maximum values are independent of its length. In our analytical model the maximum shearing stresses take place at the end planes, while the finite element analysis predicts that the maxima of these stresses are somewhat shifted from the ends. However, the maxima evaluated on the basis of the analytical stress model and the finite-element-method are in good agreement, especially for long cylinders.

The *thermally induced radial pressures* (stresses) at the end cross-sections are independent of the cylinder length. Naturally, in short cylinders they remain constant along the cylinders, so that the stresses in the inner portions of the cylinder are also length-independent. For not too long cylinders the radial pressures in the inner portion of the cylinder increase with an increase in the cylinder length. However, in sufficiently long cylinders with stiff enough interfaces, the radial pressure in the mid-portion ceases to increase with a further increase in the cylinder length and remains constant over almost the entire cylinder. Only at the very ends does the pressure decrease to a lower value. The calculated average radial pressures are in quite good agreement with the finite-element-method predictions.

The *shearing stresses due to an external shear load*, unlike thermally induced shearing stresses, are symmetric with respect to the mid-cross-section and are not zero at this cross-section, but they do reach their minimum value there. The maxima of the shearing stresses take place at the end planes, as is also the case with the thermally induced stresses. For short enough cylinders with sufficiently compliant interfaces the shearing stresses caused by external loading are distributed more or less evenly along the cylinder. When the cylinder length increases, the stresses in the inner part of the cylinder decrease, while the stresses in the end portions go up. For long cylinders with stiff interfaces the stresses concentrate near the cylinder ends, as in the case of thermally induced stresses. The minimum values of the externally induced stresses in the inner part of long-and-stiff cylinders are close to zero, and the maxima at the ends become independent of the cylinder length and are determined by the applied force (per unit circumferential length at the interface), and by the axial interfacial stiffness of the cylinder.

A bi-annular cylinder fabricated at an elevated temperature and subjected to an external shearing load at a lower, say, room temperature, experiences both thermally and externally induced stresses. The total shearing stress can be evaluated by superimposing the anti-symmetric thermal stresses and the symmetric externally induced stresses. It is this maximum total stress which is responsible for the ultimate adhesive strength at the interface. In our numerical example, which was carried out for strongly mismatched materials (coefficients of thermal expansion for the inner and the outer materials are $2.8 \times 10^{-6}/^{\circ}C$ and $22.0 \times 10^{-6}/^{\circ}C$, respectively), the maximum thermal shearing stresses in a 0.5 in (12.7 mm) long cylinder were about 6.5 times greater than the maximum stresses caused by destructive external loading (i.e. by loading resulted in an adhesive failure of the bi-annular cylinder).

If destructive shearing tests ("shear off" tests) are performed and the total force F_t and friction force F_f are measured (these can be obtained from the "force vs time" diagram), then the adhesive force F_a can be determined as the difference between the above forces. Our theory enables one to evaluate the magnitude and the distribution of the ultimate shearing stresses due to the force F_a and, using the calculated thermally induced stresses, determine the total shearing stress due to the combined action of the thermally induced and external forces.

As a by-product of this theory, the friction coefficient between the cylinder materials can be determined for different temperature conditions. This can be done as a result of dividing the friction force obtained from Instron testing by the calculated total lateral force due to the normal thermally induced interfacial pressure.

In conclusion, we would like to emphasize that although our theory has been developed for a rather narrow problem of materials science, it has a quite broad scope of applications. Examples are: insulated tubes and electrical wires; coated optical fibers; high-pressure vessels; shaft-hub joints in gears, turbines and propellers; and even barrels of artillery guns.

Acknowledgements—The authors acknowledge fruitful discussions with P. Hubbauer, S. Matsuoka, L. T. Manzione, and J. M. Segelken. The help of H. E. Bair and D. J. Boyle who provided the materials data is greatly appreciated as is the contribution of S. W. Kulba who molded the test specimens.

REFERENCES

Filon, L. (1902). On the elastic erquilibrium of circular cylinders under certain practical systems of loads. *Phil. Trans. Soc., London*. Ser. A, 198.

Hetnarski, R. B. ed. (1986). *Thermal Stresses*. North-Holland, Amsterdam.

Lurie, A. J. (1955). *Three-dimensional Problem of the Theory of Elasticity* (in Russian). Gostekhizdat, Moscow.

Suhir, E. (1986). Stresses in bi-metal thermostats. *J. Appl. Mech.* **53**, 657–660.

Takeuti, Y., Ishida, R. and Tanigawa, Y. (1983). On an axisymmetric coupled thermal stress problem in a finite circular cylinder. *J. Appl. Mech.* **50**, 116–122.

Timoshenko, S. P. (1959). *Theory of Elasticity*. McGraw-Hill, Scarborough, CA.

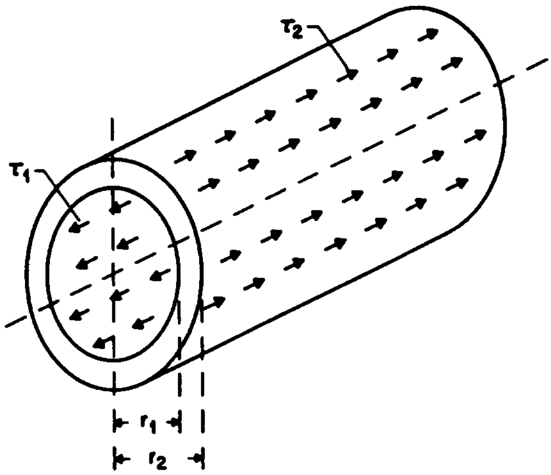

Fig. A1.

APPENDIX A

Displacements in a cylinder loaded by axial shearing forces

Examine a cylinder, loaded by uniformly distributed axial shearing forces (Fig. A1). The boundary conditions are as follows:

$$\sigma_r = 0, \quad \tau_{rz} = \tau_1 \quad \text{when } r = r_1 \tag{A1}$$

$$\sigma_r = 0, \quad \tau_{rz} = \tau_2 \quad \text{when } r = r_2. \tag{A2}$$

We assume that the radial and the the tangential normal stresses σ_r and σ_θ are zero everywhere, that the shearing stresses τ_{rz} depend on the radius r only, and that the axial normal stresses σ_z depend on the longitudinal coordinate z only. Then the condition of equilibrium (see, for instance, Timoshenko, 1959)

$$\frac{\partial \sigma_r}{\partial r} + \frac{\partial \tau_{rz}}{\partial z} + \frac{\sigma_r - \sigma_\theta}{r} = 0$$

for the radial forces is fulfilled automatically, and the condition of equilibrium

$$\frac{\partial}{\partial r}(r\tau_{rz}) + r\frac{\partial \sigma_z}{\partial z} = 0$$

for the axial forces results in the following ordinary differential equation:

$$\frac{1}{r}\frac{\mathrm{d}}{\mathrm{d}r}(r\tau_{rz}) = -\frac{\mathrm{d}\sigma_z}{\mathrm{d}z}.$$

Since the left part of this equation is z independent, and the right part is r independent, we conclude, that

$$\frac{1}{r}\frac{\mathrm{d}}{\mathrm{d}r}(r\tau_{rz}) = 2Co, \quad \frac{\mathrm{d}\sigma_z}{\mathrm{d}z} = -2Co$$

where Co is constant. By integrating these equations we obtain:

$$\tau_{rz} = C_0 r + C_1 r^{-1}, \quad \sigma_z = -2C_0 z + C_2$$

where C_1 and C_2 are constants of integration. After substituting the obtained formula for τ_{rz} into the boundary conditions (A1) and (A2) we find:

$$r_1 C_0 + r_1^{-1} C_1 = \tau_1, \quad r_2 C_0 + r_2^{-1} C_1 = \tau_2.$$

Then we obtain:

$$C_0 = \frac{\tau_2 r_2 - \tau_1 r_1}{r_2^2 - r_1^2}, \quad C_1 = \frac{\tau_2 r_1 - \tau_1 r_2}{r_2^2 - r_1^2} r_1 r_2$$

and shearing stresses are expressed as follows:

$$\tau_{rz} = \frac{(\tau_2 r_2 - \tau_1 r_1) r + (\tau_2 r_1 - \tau_1 r_2) r_1 r_2 r^{-1}}{r_2^2 - r_1^2}.$$

The constant C_2 can be put equal to zero, since there are no equilibrating loads applied at the end cross-sections. Therefore the longitudinal normal stress is:

$$\sigma_z = -\frac{2}{r_2^2-r_1^2}(\tau_2 r_2-\tau_1 r_1)z.$$

In order to determine the displacements, we use the following equations for the strains (see Timoshenko, 1959):

$$\left.\begin{aligned}
\varepsilon_r &= \frac{\partial u}{\partial r} = \frac{1}{E}[\sigma_r-\nu(\sigma_z+\sigma_\theta)] = -\frac{\nu}{E}\sigma_z = \frac{2\nu}{E}\frac{\tau_2 r_2-\tau_1 r_1}{r_2^2-r_1^2}z \\
\varepsilon_\theta &= \frac{u}{r} = \frac{1}{E}[\sigma_\theta-\nu(\sigma_z+\sigma_r)] = -\frac{\nu}{E}\sigma_z = \frac{2\nu}{E}\frac{\tau_2 r_2-\tau_1 r_1}{r_2^2-r_1^2}z \\
\varepsilon_z &= \frac{\partial w}{\partial z} = \frac{1}{E}[\sigma_z-\nu(\sigma_r+\sigma_\theta)] = \frac{\sigma_z}{E} = -\frac{2}{E}\frac{\tau_2 r_2-\tau_1 r_1}{r_2^2-r_1^2}z \\
\gamma_{rz} &= \frac{\partial u}{\partial z}+\frac{\partial v}{\partial r} = \frac{\tau_{rz}}{G} = \frac{2(1+\nu)}{G}\frac{(\tau_2 r_2-\tau_1 r_1)r+(\tau_2 r_1-\tau_1 r_2)r_1 r_2 r^{-1}}{r_2^2-r_1^2}
\end{aligned}\right\} \tag{A3}$$

From the second equation we obtain:

$$u = \frac{2\nu}{E}\frac{\tau_2 r_2-\tau_1 r_1}{r_2^2-r_1^2}rz. \tag{A4}$$

Then the first equation is also fulfilled. The third equation in (A3) yields:

$$w = \frac{1}{E}\frac{\tau_2 r_2-\tau_1 r_1}{r_2^2-r_1^2}z^2+\Delta w(r) \tag{A5}$$

where $\Delta w(r)$ is an arbitrary function of the radius r. After substituting (A5) and (A4) into the last formula in (A3) we obtain the following equation for this function:

$$\frac{\mathrm{d}(\Delta w(r))}{\mathrm{d}r} = \frac{2}{E}\frac{(\tau_2 r_2-\tau_1 r_1)r+(1+\nu)(\tau_2 r_1-\tau_1 r_2)r_1 r_2 r^{-1}}{r_2^2-r_1^2}.$$

Then we have:

$$\Delta w(r) = \frac{1}{E}\frac{(\tau_2 r_2-\tau_1 r_1)r^2+2(1+\nu)(\tau_2 r_1-\tau_1 r_2)r_1 r_2 \ln r}{r_2^2-r_1^2}, \tag{A6}$$

where the constant of integration is put equal to zero, since it does not result in any elastic strains.

Note, that if the force

$$T(z) = 2\pi(r_1\tau_1-r_2\tau_2)z$$

acting in the z cross-section, were uniformly distributed over the cross-sectional area, then the axial displacements, calculated in accordance with Hooke's law, would be

$$w = \int_0^z \frac{T(\zeta)\,\mathrm{d}\zeta}{\pi(r_2^2-r_1^2)E} = \frac{\tau_1 r_1-\tau_2 r_2}{E(r_2^2-r_1^2)}z^2$$

for all the points of this cross-section. Comparing this formula with (A5) we conclude that the function $\Delta v(r)$ accounts for the additional axial displacements due to the nonuniform distribution of the internal loads.

When the shearing stress is applied to the outer surface only ($\tau_1 = 0$) the formula (A6) yields:

$$\Delta w(r) = \frac{\tau_2 r_2}{E}\frac{r^2+2(1+\nu)r_1^2 \ln r}{r_2^2-r_1^2}.$$

This formula can be used for the evaluation of the axial interfacial compliance of the inner cylinder in a bi-annular cylinder. Putting $E = E_0$, $\nu = \nu_0$, $r_1 = r_0$, $r_2 = r_1$, and $\tau_2 = \tau$, we have:

$$\Delta w(r) = \frac{\tau r_1}{E_0}\frac{r^2+2(1+\nu_0)r_0^2 \ln r}{r_1^2-r_0^2}.$$

The relative axial displacement of the points located on the outer surface ($r = r_1$) and in the mid-surface

$$\left(r = \bar{r}_0 = \frac{r_0+r_1}{2}\right)$$

of the cylinder is

$$\Delta(\Delta w) = \Delta w(r_1)-\Delta w(\bar{r}_0) = \frac{\tau r_1}{E_0}\frac{r_1^2-\bar{r}_0^2+2(1+\nu_0)r_0^2 \ln(r_1/\bar{r}_0)}{r_1^2-r_0^2}$$

so that the compliance coefficient is

$$\kappa_0 = \frac{\Delta(\Delta w)}{\tau} = \frac{r_1}{E_0(r_1^2-r_0^2)}\left[r_1^2-\bar{r}_0^2+2(1+\nu_0)r_0^2\ln\frac{r_1}{\bar{r}_0}\right]. \tag{A7}$$

In the case when the shearing stress in applied to the inner surface only ($\tau_2 = 0$) the formula (A6) yields:

$$\Delta w(r) = -\frac{\tau_1 r_1}{E}\frac{r^2+2(1+\nu)r_2^2\ln r}{r_2^2-r_1^2}.$$

Putting in this formula $E = E_1$, $\nu = \nu_1$, $\tau_1 = \tau$, and evaluating the relative axial displacement of the points located on the inner surface ($r = r_1$) and in the mid-surface

$$\left(r = \bar{r}_1 = \frac{r_1+r_2}{2}\right)$$

of the outer cylinder, we obtain the following formula for the axial interfacial compliance:

$$\kappa_1 = -\frac{\Delta(\Delta w)}{\tau} = \frac{r_1}{E_1(r_2^2-r_1^2)}\left[\bar{r}_2^2-r_1^2+2(1+\nu_1)r_2^2\ln\frac{\bar{r}_2}{r_1}\right]. \tag{A8}$$

APPENDIX B

Axial displacements due to lateral pressures

The radial and the tangential (circumferential) stresses in a thick-walled tube subjected to an internal (p_i) and external (p_o) pressures can be evaluated by the formulas (see, for instance, Timoshenko, 1959):

$$\left.\begin{aligned}\sigma_r &= \frac{1}{b^2-a^2}\left[\frac{a^2b^2}{r^2}(p_op_i)-(p_ob^2-p_ia^2)\right]\\ \sigma_\theta &= \frac{1}{b^2-a^2}\left[-\frac{a^2b^2}{r^2}(p_o-p_i)-(p_ob^2-p_ia^2)\right]\end{aligned}\right\}, \tag{B1}$$

where a and b are the inner and the outer radii of the cylinder. From these formulas we have:

$$\sigma_r+\sigma_\theta = \frac{2}{b^2-a^2}(p_ob^2-p_ia^2). \tag{B2}$$

The axial normal strains are expressed in the axisymmetrical problem of the elasticity theory as follows (Timoshenko, 1959):

$$\varepsilon_z = \frac{\partial w}{\partial z} = \frac{1}{E}[\sigma_z-\nu(\sigma_r+\sigma_\theta)]$$

where σ_z is the axial stress, and w is the axial displacement. As evident from this formula, the axial displacement due to the lateral stresses σ_r and σ_t is

$$w = -\frac{\nu}{E}\int_0^z(\sigma_r+\sigma_\theta)\,dz.$$

After introducing (B2) into this formula we have:

$$w = \frac{2\nu}{E}\frac{p_ob^2-p_ia^2}{b^2-a^2}z.$$

In the case of an inner cylinder $E = E_0$, $\nu = \nu_0$, $p_i = 0$, $p_0 = p$, $a = r_0$, and $b = r_1$, so that

$$w = \frac{2\nu_0}{E_0}\frac{r_1^2}{r_1^2-r_0^2}pz. \tag{B3}$$

In the case of an outer cylinder $E = E_1$, $\nu = \nu_1$, $p_i = p$, $p_0 = 0$, $a = r_1$, and $b = r_2$, and therefore

$$w = \frac{2\nu_1}{E_1}\frac{r_1^2}{r_2^2-r_1^2}pz. \tag{B4}$$

APPENDIX C

Radial displacements due to the radial and axial interfacial loading

If the cylinder is sufficiently short, and the plane stress approximation should be applied, then the following formula for the radial displacements is used (see, for instance, Timoshenko, 1959):

$$u = \frac{1}{E(b^2-a^2)}\left[(1-\nu)(p_i a^2 - p_o b^2)r - 1(1+\nu)(p_o - p_i)\frac{a^2b^2}{r}\right].$$

The notation here is the same as in the Appendix B. In the case of an inner cylinder $E = E_0$, $\nu = \nu_0$, $p_i = 0$, $p_0 = p$, $a = r_0$, $b = r_1$, *and* $r = r_1$. Thus we have:

$$u = -\frac{pr_1}{E_0(r_1^2-r_0^2)}[(1-\nu_0)r_1^2+(1+\nu_0)r_0^2]. \tag{C1}$$

In the case of an outer cylinder, putting $E = E_1$, $\nu = \nu_1$, $p_i = p$, $p_o = o$, $a = r_1$, $b = r_2$, and $r = r_1$, we obtain:

$$u = \frac{pr_1}{E_1(r_2^2-r_1^2)}[(1-\nu_1)r_1^2+(1+\nu_1)r_2^2]. \tag{C2}$$

For relatively long cylinders when the plane strain approximation is used, the elastic constants E and ν in the above formulas should be substituted by

$$\frac{E}{1-\nu^2} \quad \text{and} \quad \frac{\nu}{1-\nu},$$

respectively. This results in the formula:

$$u = -\frac{pr_1(1+\nu_0)}{E_0(r_1^2-r_0^2)}[(1-2\nu_0)r_1^2+r_0^2] \tag{C3}$$

for the inner cylinder and in the formula

$$u = \frac{pr_1(1+\nu_1)}{E_1(r_2^2-r_1^2)}[(1-2\nu_1)r_1^2+r_2^2] \tag{C4}$$

for the outer cylinder.

The radial displacements due to the axial loading can be determined on the basis of the formula (Timoshenko, 1959)

$$\varepsilon_\theta = \frac{u}{r} = \frac{1}{E}(\sigma_t - \nu\sigma_r - \nu\sigma_z)$$

for the tangential strain. As evident from this formula, the radial displacements caused by the axial stress σ_z are as follows:

$$u = -\frac{\nu}{E}\sigma_z r.$$

The axial stresses in the inner cylinder are

$$\sigma_z = -\frac{T(z)}{\pi(r_1^2-r_0^2)} = -\lambda_0 E_0 T(z)$$

and therefore the radial interfacial displacements ($r = r_1$) can be evaluated by the formula

$$u = \nu_0\lambda_0 r_1 T(z). \tag{C5}$$

The axial stresses in the outer cylinder are

$$\sigma_z = \frac{T(z)}{\pi(r_2^2-r_1^2)} = \lambda_1 E_1 T(z)$$

so that the radial interfacial displacements are expressed as:

$$u = -\nu_1\lambda_1 r_1 T(z). \tag{C6}$$